Radar observations of seasonal snow in an agricultural field in S. Ontario during the 2013-2014 winter season

Aaron Thompson, Richard Kelly and Andrew Kasurak

Interdisciplinary Centre on Climate Change and

Department of Geography and Environmental Management

University of Waterloo

Waterloo, ON, N2L 3G1, Canada

ABSTRACT

Recent studies of radar observations of moderate snow depth have been conducted in sub-Arctic and mountain environments but less so over seasonal mid-latitude snow. Radar observations of snow at Ku- and X-band were made in an agricultural field near Maryhill Ontario during the 2013-2014 winter season. In each deployment, the natural snowpack was scanned and then fully excavated; a scan of the bare, underlying soil followed. In-situ measurements of the snow properties accompanied the radar observations. In cold, dry conditions, it was observed that Ku-band showed sensitivity to the presence of snow and the radar response increased with snow water equivalent (SWE). Sensitivity to snow in the same conditions was not observed at X-band. In the presence of warm air temperatures and snow melt, an increase in backscatter was observed at both frequencies and little difference was observed between the snow and no-snow condition. This was due to the unique combination of warm air temperatures, melting snow and ice layers in the snowpack that enhanced surface scattering.

INTRODUCTION

Snow is an important component of the annual terrestrial water cycle. Characterizing and quantifying snow state is important for water resource management and energy budget modelling (Rott et al., 2010). Run-off from snow melt provides fresh water for aquatic ecosystems, agriculture, industry, and municipal water supply (Pomeroy et al., 2009). Furthermore, long-term snow mapping studies provide insights into the nature of snow as an indicator of climate change (Brown & Mote, 2009). Given its importance, changes in snow extent, duration, and distribution

due to climate change have emphasized the need for a practical system of monitoring (Morrison et al., 2007; Rott et al., 2010). This has prompted organizations such as the World Meteorological Organization and the Integrated Global Observing Strategy to articulate the need for high-resolution snow water equivalent (SWE) observations (Rott et al., 2012b; Yueh et al., 2009).

Radar remote sensing of snow is a practical means of obtaining information on seasonal snowpack accumulation at high spatial and temporal resolution (Rott et al., 2010). Studies have identified microwave frequencies of 8-18 GHz as being sensitive to snow volume (King et al., 2013, Morrison et al., 2007; Yueh et al., 2009). In particular, a Ku-band sensitivity to SWE has been observed (King et al., 2013). Studies in the European Alps, sub-Arctic Scandinavia and Canada have demonstrated a strong relationship between Ku-band scatterometer observations and SWE. However, observations of SWE in mid-latitude continental snowpacks dominated by low pressure cyclones and lake-effect snow have not been tested using Ku- and X-band observations. The overall aim of this study is to explore the applicability of Ku- and X-band scatterometer measurements of snow near Maryhill, Ontario, which is subject to lake effect snow and systematic cyclonic winter storm activity. The objectives are to: 1) understand the backscatter radar response from seasonal lake effect snow, 2) understand the polarimetric radar response at Ku- and X-band in this environment, and 3) develop a field data set to test microwave scattering models for moderate snow accumulation in open field environments.

STUDY AREA

The study area was located in a cut hay field near Maryhill, Ontario (80°22.75'W 43°32.89'N) and was situated on Guelph Loam (Ontario Ministry of Agriculture, Food, and

Rural Affairs, 2000). Figure 1 shows the study area and locations of observation sites and the meteorological station.

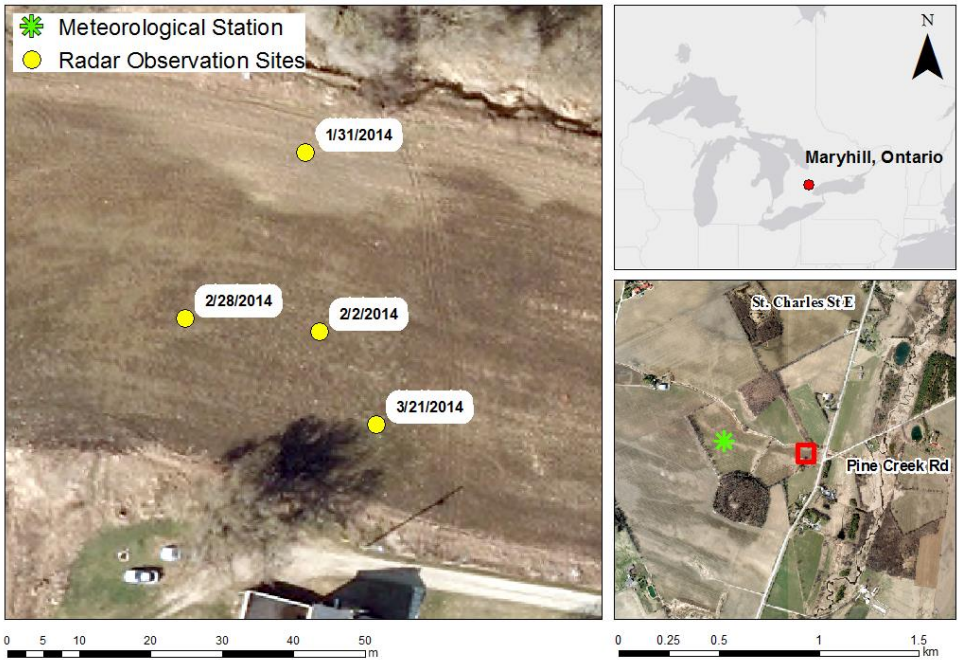

Figure 1. Study area near Maryhill Ontario, showing radar observation sites (Environmental Systems Research Institute, 2014; Ontario Ministry of Natural Resources, 2010).

The ground was level with furrows of approximately 5 cm depth and 55 cm spacing (Figure 2) arranged in an east-west orientation; there was little variation in topography along the furrows. Between January and March, 2014, the study area was visited on four occasions and each time, a new observation site within the field was chosen based on variation in snowpack conditions.

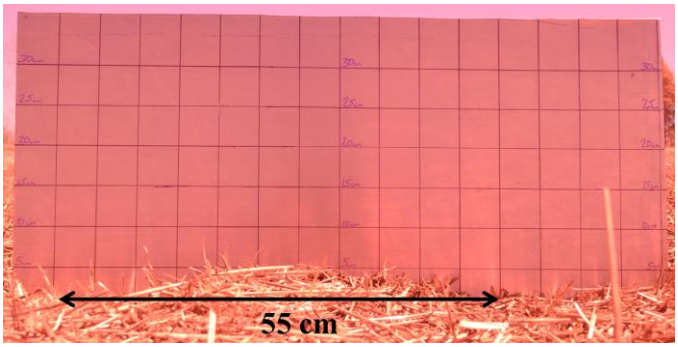

Figure 2. Photograph of surface topography at observation sites showing 55 cm furrow spacing and 5 cm depth. Grid cells on backdrop are 5x5 cm.

DATA & METHODS

The field observations were collected on January 31, February 2, February 28 and March 21. They included radar observations of the snowpack and *in situ* observations of snow properties. *In situ* observations from snow pits included snow depth, density, temperature and grain size measurements, and stratigraphy observations augmented with infrared photography. A nearby meteorological station recorded air temperature, wind speed, relative humidity, and radiation at the site.

Each date corresponded with different snow depths, snowpack characteristics and weather conditions, although an attempt was made to perform scans on cold days and during periods with sustained antecedent air temperatures less than -10°C to avoid the presence of liquid water in the snowpack. On each visit, the soil was frozen although on March 21, the air temperature was above 0°C and the soil surface began to thaw once the snow was excavated.

Radar observations were made with a ground-based polarimetric scatterometer at both X- and Ku-band frequencies (9.6 and 17.2 GHz respectively) in a narrow-beam mode configuration. Backscatter measurements were made using a combination of vertical (V) and horizontal (H)

send-receive polarization states, reflected by the co-polarized terms VV and HH, and the cross-polarized terms VH and HV. A detailed description of this equipment, including its specifications and calibration procedures, can be found in King et al. (2013). Observation sites were selected such that they were on level ground, away from hills or ditching, and to ensure a range of snow depths. The radar was tripod-mounted on top of the snow surface. We prevented the tripod from settling into the snow by locating plywood squares beneath each foot to distribute the load; this also facilitated levelling of the equipment since it stabilized the platform. This configuration placed the antenna at 2.2 m above the snow surface. In order to collect backscatter measurements, the scans were conducted over a 27° range in elevation with incident angles of 35° to 62°, in 3° increments, and a 20° azimuth sweep centred at 0°. Each scan was repeated 3 times and averaged in order to minimize the effects of system noise. From the backscatter measurements, depolarization and polarization ratios were calculated which provide insight into the geometrical properties of the target (Woodhouse, 2006). The depolarization ratio was calculated as follows, where σ^o represents the measured backscatter for each send-receive polarization:

$$r_{depolarization} = \frac{\sigma^o_{VV}}{\sigma^o_{VH}} \quad (1)$$

This ratio provides an indication of how much depolarization occurs as a result of interaction with the snowpack or the bare ground. The polarization ratio compares the vertical and horizontal contributions to the signal:

$$r_{polarization} = \frac{\sigma^o_{VV}}{\sigma^o_{HH}} \quad (2)$$

It provides information on the nature and orientation of the scattering centres within the target.

On each day, two sets of scans were performed. In the first set of scans, the naturally occurring snowpack was observed at both frequencies. For the second set of scans, all the snow within a 5 m by 5 m area in front of the scatterometer was excavated to bare soil. The excavated area was oriented such that the scatterometer was located at the midpoint of one side facing towards the snow-free soil. The scans were repeated for both frequencies using the same parameters and positioning as before. The equipment configuration can be seen in Figure 4. Because the air and soil temperatures remained below freezing during the study period, excluding March 21, the condition of the underlying soil was assumed to have remained constant. For this reason, the backscatter for the excavated sites (except for March 21) was averaged to represent the snow-free condition.

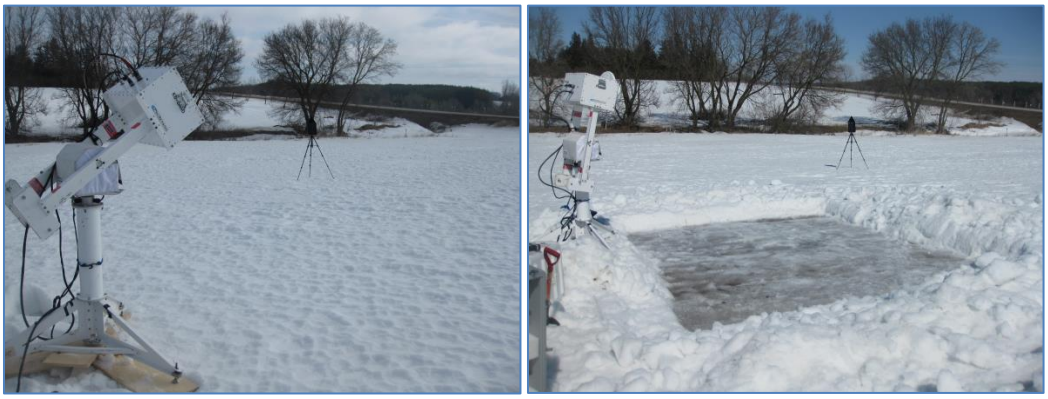

Figure 3 Scatterometer configuration shown. At left, natural snow cover is being scanned. At right the excavated area can be seen.

In between the two sets of scans, before the snow was excavated, snow depths were recorded over a 10 m by 10 m area in front of the scatterometer. The measurements were made in a grid with 50 cm spacing, using a Magnaprobe. An exception to this grid spacing was made 2 m directly in front of the scatterometer where a 1 m^2 area was left undisturbed for the snow pit.

Before the snow was entirely excavated, the snow pit was dug in the radar's field of view. Snowpack stratigraphy was observed and the pit face was photographed using a Nikon D90 camera with a 1000 nm infrared filter. Grain size estimates were made of samples from each layer using a pocket microscope and measurement card with 1 and 3 mm grids. Snow samples were taken from the pit wall, spanning the vertical extent of face, using a 100 cm^3 density cutter. These samples were weighed immediately and discarded; density was calculated using the weight and volume. Temperature was also measured with a mechanical probe at each layer of the snowpack, including the air-snow interface and snow-soil interface. SWE was calculated from the density and depth measurements.

RESULTS

Table 1 summarizes the snowpack conditions for each observation period. The density was greatest on March 20, at 420 kg/m^3 which corresponded with warm air temperatures and snow melt. Snow density measurements for February 28 were not available so SWE was calculated for this date using the snow density measurement from February 2.

Table 1. Summary of snowpack conditions by date.

DATE	Snow Depth (cm)	Snow Density (kg/m3)	SWE (mm)
January 31, 2014	40	344	138
February 2, 2014	28	287	80
February 28, 2014	55	287	160
March 21, 2014	23	420	97

Air temperature for the observation period is provided in Figure 4. Each observation occurred during a period of sustained sub-freezing air temperatures except for the March 21 observation at which time the air temperature had risen above 0°C.

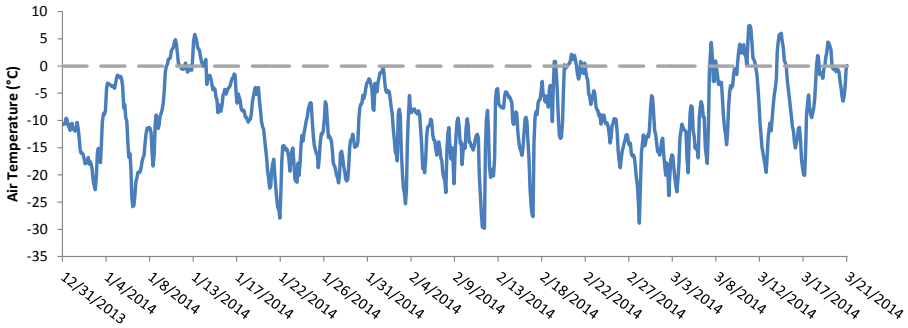

Figure 4. Air temperature for the observation period.

A comparison of backscatter over the range of elevation angles for snow and no-snow conditions for varying SWE at both frequencies is shown in Figure 5. At Ku-band, the backscatter for the no-snow condition is generally 5-8 dB lower than that of the snow-covered condition. This is especially visible for the co-polarized response at 138 and 154 mm SWE. At 97 mm SWE there was little difference between the snow-on and snow-off condition. At X-band, there was also little observable difference between the snow-on and snow-off condition. In all cases, backscatter appears to decrease with increasing elevation angle.

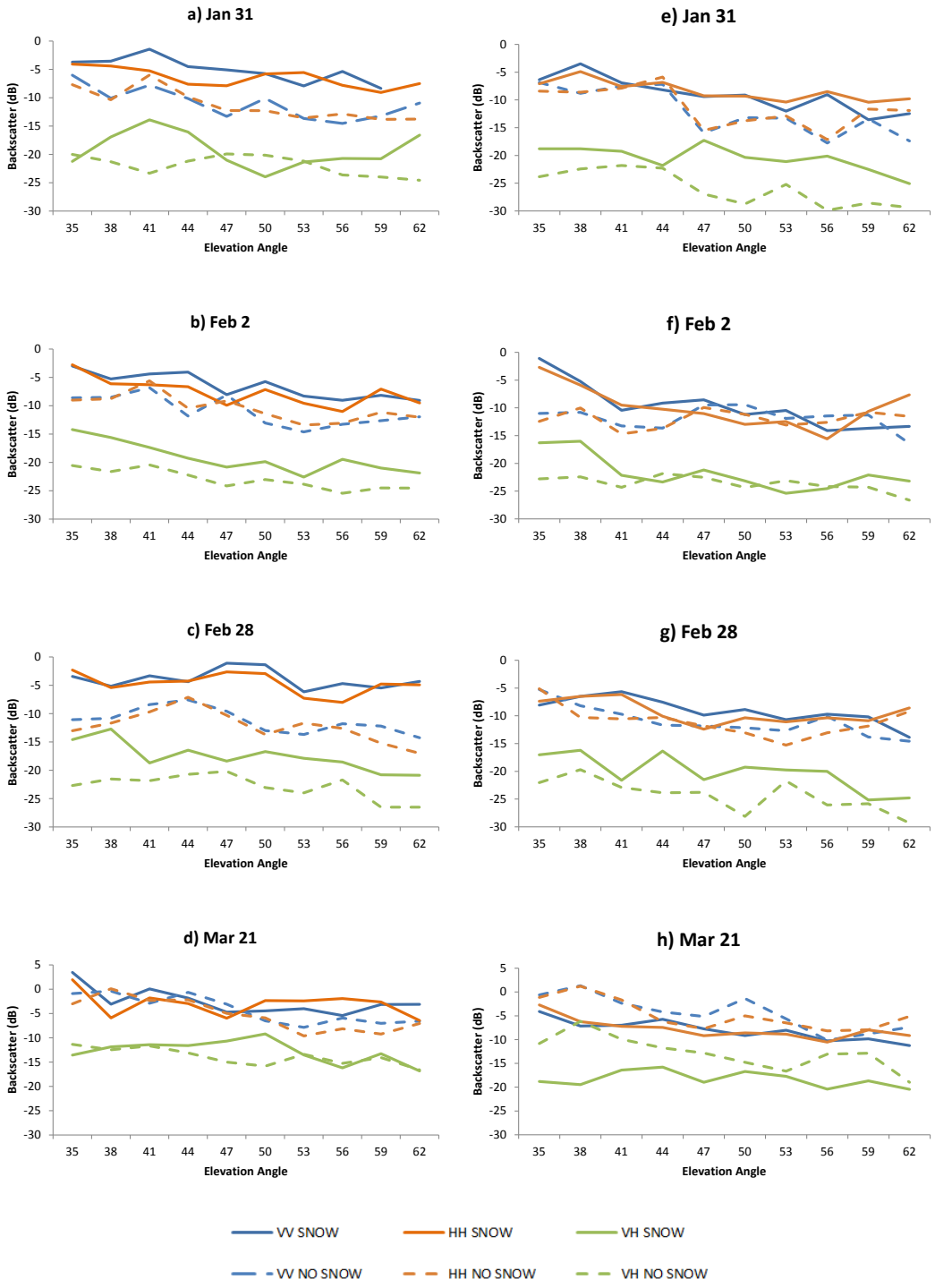

Figure 5. Backscatter over range of elevation angles for snow and no-snow conditions at Ku-band (a-d) and X-band (e-h).

The relationship between SWE and backscatter is plotted in Figure 6 for backscatter averaged over elevation angles of 47° to 56°. At Ku-band there was an increase of nearly 10 dB between 0 and 138 mm SWE for the co-polarized return; there appears to be less change for the

cross-polarized return. At X-band, an increase in backscatter with SWE was much less apparent. From 0 to 138 mm SWE there was an increase of about 3 dB

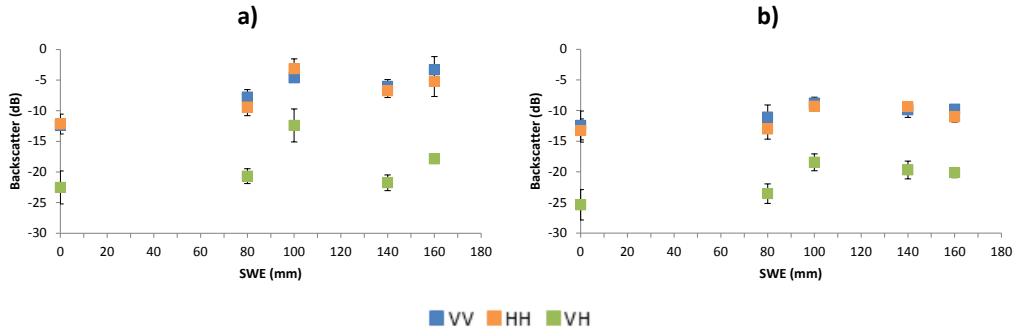

Figure 6. Comparison of backscatter and SWE at Ku-band (a) and X-band (b). Error bars represent 1 standard deviation.

Depolarization ratios are shown in Figure 7. At Ku-band, the ratio for the no-snow condition was always greater than for the snow condition due to a stronger co-polarized response in the presence of snow; on March 21 this pattern was reversed beyond an elevation angle of 50°. For X-band, there was little difference between ratios for the snow and no-snow condition, except on March 21 where the no-snow condition exhibited strong variability in ratio across the elevation angles. The depolarization ratio was also calculated for HH polarization but the outcome was similar therefore only the ratio incorporating VV polarization was reproduced here.

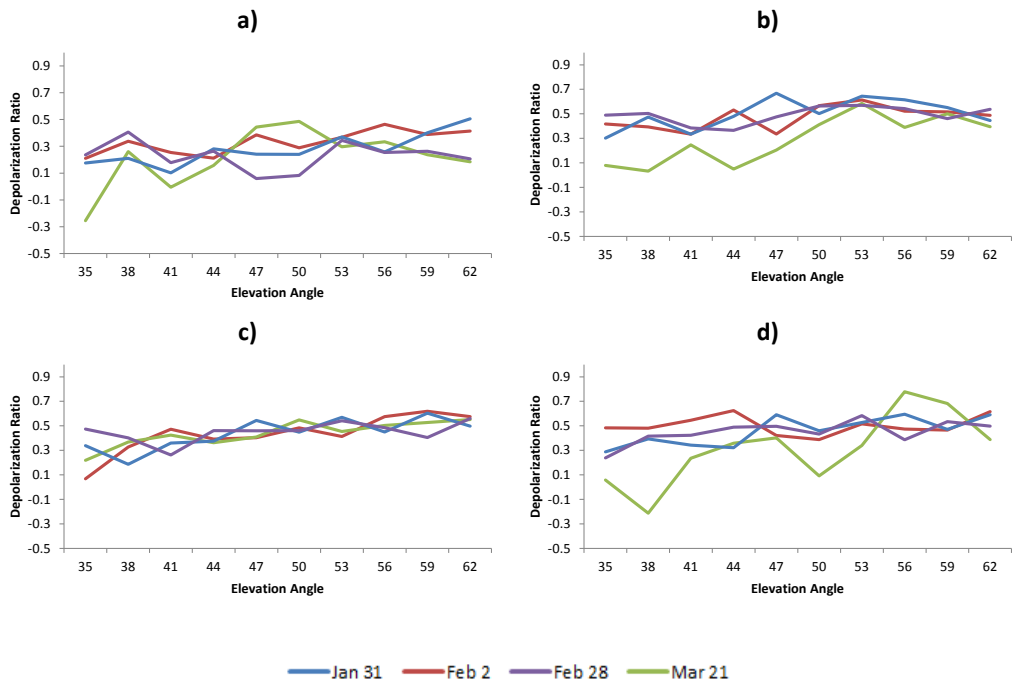

Figure 7. Depolarization ratios at Ku-band for snow (a) and no-snow (b) conditions, and at X-band for snow (c) and no-snow (d) conditions.

The polarization ratios provided in Figure 8 show separation between the snow and no-snow condition at Ku-band whereby the ratio for the snow condition was generally less than that of the no-snow condition, and usually maintained a value below 1; the VV response was typically stronger than the HH response. The ratio for the no-snow condition varied around 1 indicating the VV and HH responses were similar. There was very little separation at X-band and the ratio varied around 1.

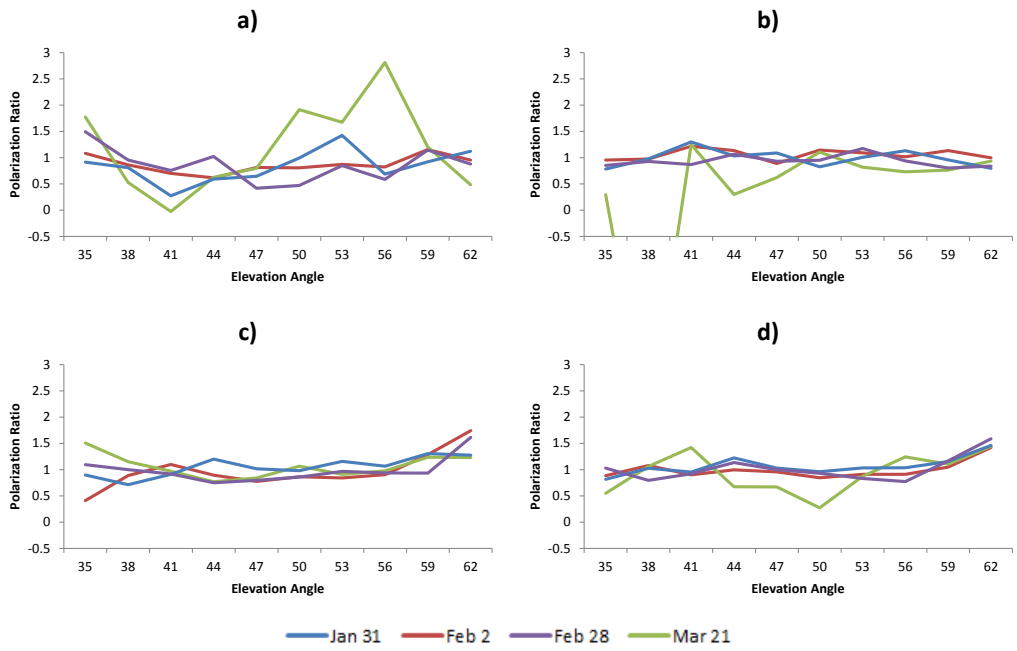

Figure 8. Polarization ratios at Ku-band for snow (a) and no-snow (b) conditions, and X-band for snow (c) and no-snow conditions (d).

DISCUSSION

Two distinct weather regimes were observed during the course of this study. The cold regime included observations from January 31, February 2, and February 28. During this period, the air temperatures were sustained below -10°C which provided a cold snowpack with no melt and therefore no liquid water content. The warm regime was observed on March 21; the snow conditions on this day were different than all other days. The snowpack was isothermal at 0°C, the air temperature was above 0°C and snow was melting, creating a wet snowpack. Upon excavation of the snow, the surface layer of the soil thawed, and residual ice melted leaving a mixed surface of standing water and thawed, wet soil. Because of the distinct differences between the cold and warm regimes, they will be discussed separately.

COLD REGIME

It was generally observed that Ku-band was more responsive to the snowpack than X-band; Figures 4 and 5 illustrate this sensitivity. There was little observable change in the X-band response when the snow was removed, and there was little change in X-band backscatter with increasing SWE. This provided strong indication that the X-band signal was a response to the underlying soil in each case while the Ku-band signal, which was observed to increase with SWE and in response to snow excavation, was a response to the snowpack. The polarization and depolarization ratios further corroborated this evidence. The depolarization ratios showed a decrease in the presence of snow due to a stronger co-polarized response while the cross-polarized response remained relatively constant in the presence or absence of snow. This showed sensitivity to snow and also suggested that the snow and the bare soil similarly influenced the depolarization of the electromagnetic energy. The polarization ratios were lower in the presence of snow at Ku-band because of a stronger VV return whereas in the absence of snow, the VV and HH returns were similar. The enhancement of the VV return suggests that a vertically oriented feature within the snowpack was present. Depth hoar formation was abundant in the snowpack during the cold regime due to the sustained low air temperatures and subsequent vertical temperature gradient within the snowpack. The vertical orientation of the resulting depth hoar crystals may have been responsible for the stronger VV return. At X-band, both ratios were very similar in the presence and absence of snow suggesting that there was little change in terms of the depolarization and scattering mechanisms between the two conditions, and therefore little sensitivity to the presence of snow; this outcome supports earlier findings by King et al. (2013) for similar levels of SWE.

WARM REGIME

The expectation of a wet snowpack is that it would decrease backscatter (Kendra et al., 1998; Ulaby et al., 1984) however this was not the case on March 21. Recalling Figure 4, the observed backscatter was 5-8 dB greater when snow was present. In a wet snowpack, the backscatter becomes strongly dependent on snow surface roughness (Ulaby et al., 1984). This can lead to greater surface scattering that outweighs the decrease in volume scattering. This phenomenon was observed by Kendra et al. (1998) in Cadillac, Michigan, and they proposed that it was an exceptional result caused by a wet snowpack, warm air temperatures, and an ice lens beneath the surface impeding drainage; the conditions on March 21 were similar, including the presence of thick ice layers. It is therefore suggested that this combination of factors lead to an increase in backscatter; the depolarization and polarization ratios also support this finding. The depolarization ratios were similar for snow and no-snow conditions at both frequencies which suggest that X- and Ku-band were interacting with the target similarly. The liquid water present at the air-snow and air-soil interfaces was responsible for this, as it created a stronger co-polarized response through enhanced surface scattering. In the excavated state, the ice particles and melt water along with a thawing soil surface layer combined to increase the surface scattering contribution of the no-snow condition to a similar effect. The polarization ratios varied around a value of 1, but exhibited substantial noise; there was no clear pattern at X-band but at Ku-band, the snow condition had a higher ratio over much of the elevation range due to a stronger HH response. Since backscatter of wet snow is influenced by the surface roughness, this suggests that the surface water enhanced the horizontal orientation of the air-snow interface producing a stronger horizontal response.

CONCLUSION

Through examination of radar backscatter measurements and associated ratios, it was observed that in cold, dry conditions the Ku-band signal was a response from the snowpack, and that the return increased with SWE for a range of 0 to 138 mm SWE. Conversely it was observed that in these conditions, X-band did not respond to the snow at these levels of SWE. On a warm day on which snow melt was prevalent, backscatter was observed to increase at both frequencies and little difference in backscatter was found between the snow and no-snow condition. Liquid water at the surface of the melting snowpack, whose drainage was impeded by underlying ice layers, and on the soil of the excavated site, lead to an increase of surface scattering and caused the elevated levels of backscatter. This has important implications for radar estimates of SWE in the ripening phase of snow. Future work should explore the sensitivity of Ku- and X-band to seasonally evolving snow and end of season melting snow to better understand how they control the radar response.

REFERENCES

Brown, R. D., & Mote, P. W. (2009). The response of northern hemisphere snow cover to a changing climate. *Journal of Climate*, *22*(8), 2124–2145. doi:10.1175/2008JCLI2665.1.

Environmental Systems Research Institute. (2014). Basemap. Redlands, California.

Kendra, J. R., Sarabandi, K., & Ulaby, F. T. (1998). Radar measurements of snow: experiment and analysis. *IEEE Transactions on Geoscience and Remote Sensing*, *36*(3), 864–879.

King, J. M. L., Kelly, R., Kasurak, A., Duguay, C., Gunn, G., & Mead, J. B. (2013). UW-Scat : a ground-based dual-frequency scatterometer for observation of snow properties. *IEEE Geoscience and Remote Sensing Letters*, *10*(3), 528–532.

Morrison, K., Rott, H., Nagler, T., Rebhan, H., & Wursteisen, P. (2007). The SARALPS-2007 measurement campaign on X and Ku-Band backscatter of snow. *2007 IEEE International Geoscience and Remote Sensing Symposium*, 1207–1210. doi:10.1109/IGARSS.2007.4423022.

Ontario Ministry of Agriculture, Food, and Rural Affairs. (2000). Soil types of Ontario. Computer file. Guelph, Ontario.

Ontario Ministry of Natural Resources. (2010). SWOOP: Orthoimagery. *Land Information Ontario.*

Pomeroy, J., MacDonald, M., DeBeer, C., & Brown, T. (2009). Modelling alpine snow hydrology in the Canadian Rocky Mountains. *Western Snow Conference 2009*.

Rott, H., Yueh, S. H., Cline, D. W., Duguay, C., Essery, R., Haas, C., … Thompson, A. (2010). Cold Regions Hydrology High-Resolution Observatory for snow and cold land processes. *Proceedings of the IEEE*, *98*(5), 752–765. doi:10.1109/JPROC.2009.2038947.

Rott, H., Cline, D. W., Duguay, C., Essery, R., Etchevers, P., Hajnsek, I., Kern, M., Macelloni, G., Malnes, E., Pulliainen, J., & Yueh, S. H. (2012). CoReH$_2$O, a dual frequency radar mission for snow and ice observations. *2012 IEEE International Geoscience and Remote Sensing Symposium*, 5550–5553.

Ulaby, Fawwaz T., Stiles, W.H., Abdelrazik, M. (1984). Snowcover influence from backscattering of terrain. *IEEE Transactions on Geoscience and Remote Sensing*, (2), 126–133.

Woodhouse, I. (2006). Introduction to microwave remote sensing. Boca Raton: CRC Press.

Yueh, S. H., Dinardo, S. J., Akgiray, A., West, R., Cline, D. W., & Elder, K. (2009). Airborne Ku-Band polarimetric radar remote sensing of terrestrial snow cover. *IEEE Transactions on Geoscience and Remote Sensing*, *47*(10), 3347–3364. doi:10.1109/TGRS.2009.2022945.